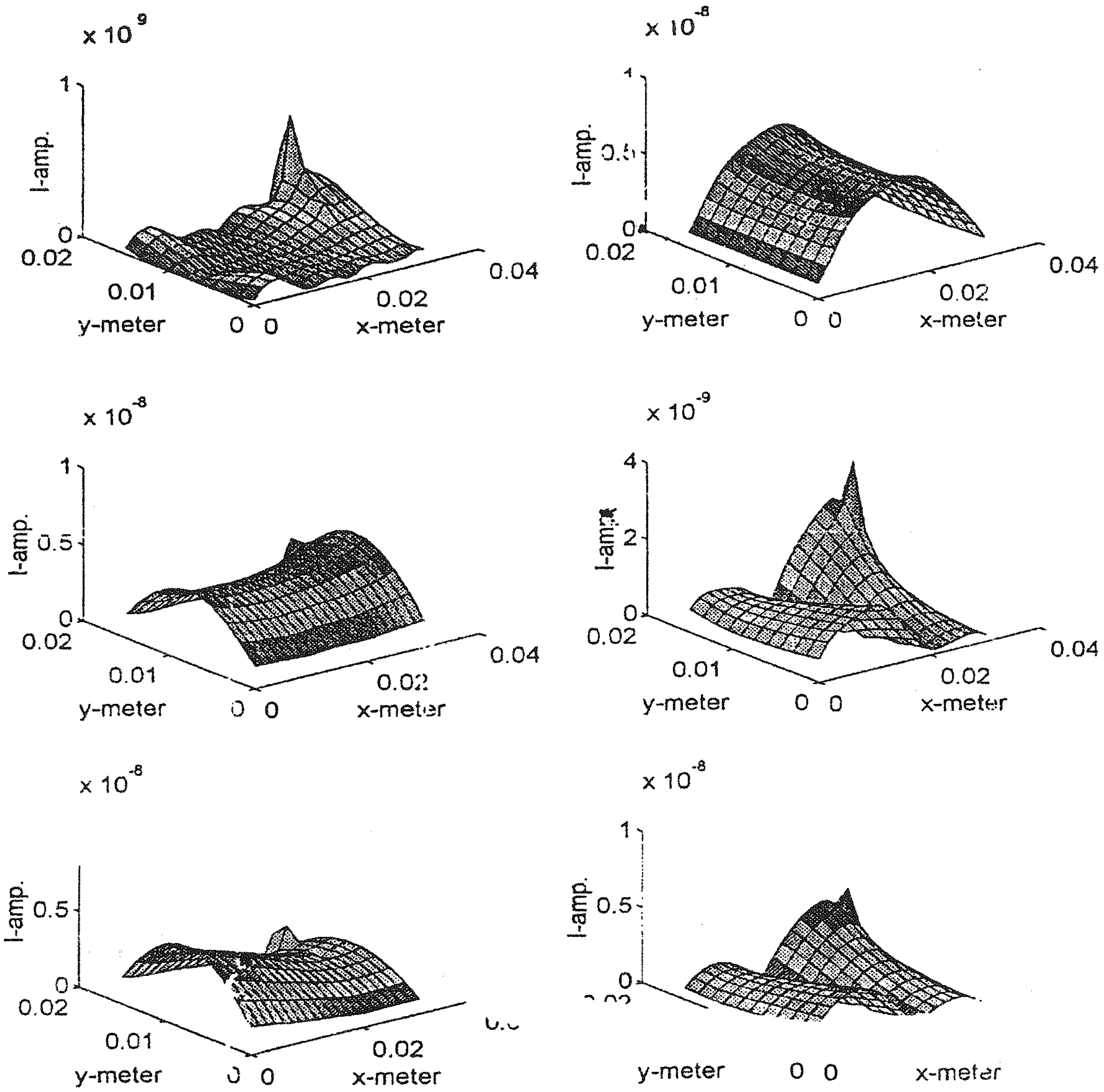

Fig (11) Current distribution

References

[1] E. H. Newman, D. Forrai, "Scattering from a Microstrip", IEEE Trans. Antennas Propagat., Vol. 35, No. 3, pp. 245-251, 1987.

[2] D. M. Pozar, " Radiation and Scattering from a Microstrip Patch on Uniaxial Substrate", IEEE Trans. Antennas Propagat., Vol. 35, No. 6 pp. 613 - 621. 1987.

[3] J. Herault, R. Moini, A. Reinex and B. Jecko, " A Mixed Analysis of Microstrip Antennas: Transient-frequency", IEEE Trans. Antennas Propagat., Vol. 38, No. 8, pp. 1166 - 1176, 1990.

[4] R. Moini"Antennas,Radon Con Sedion of tinortip patch antennas, a Single Element and Arrays", In Proc. ICEE 1993, Tehran, Iran, May 18-21, pp. 46-53, 1993.

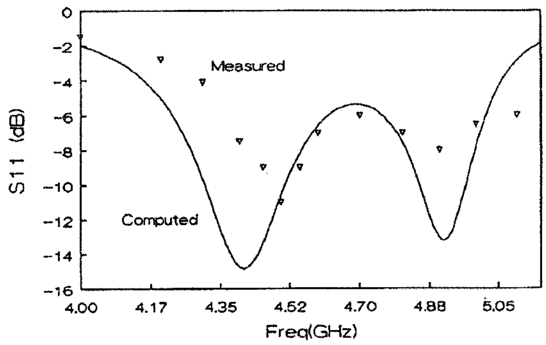

Fig (5) Reflection coefficient

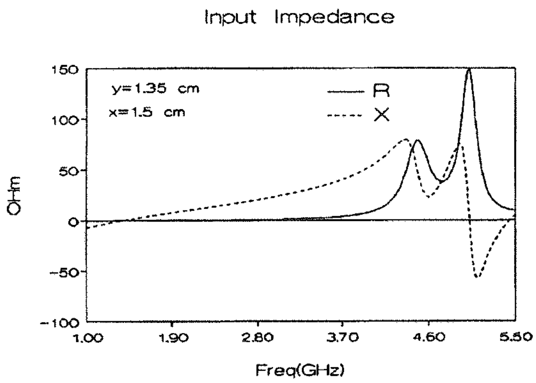

Fig (8) Input impedance

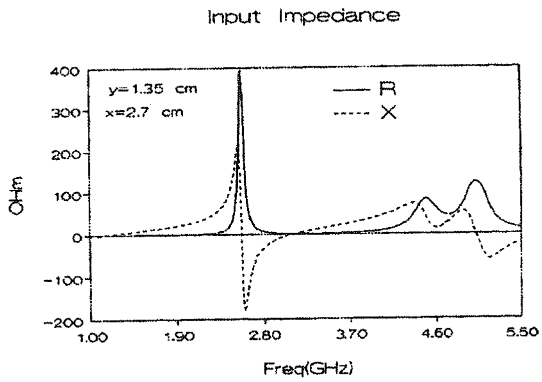

Fig (6) Input impedance

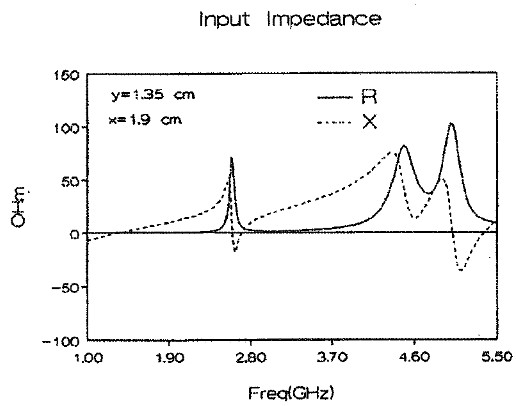

Fig (9) Input impedance

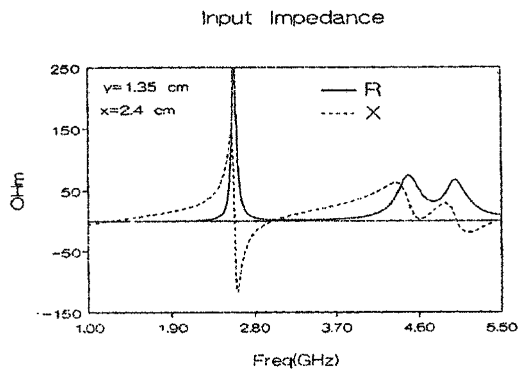

Fig (7) Input impedance

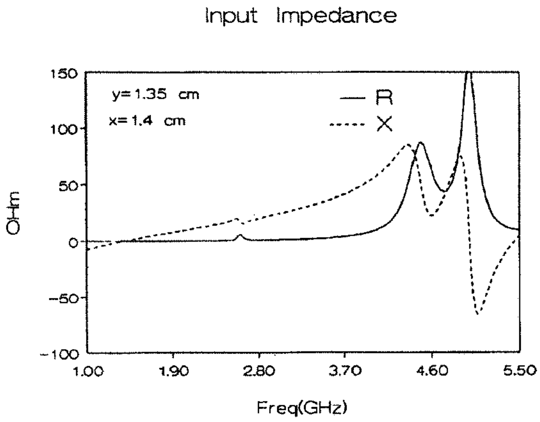

Fig (10) Input impedance

Figure 11 depicts the current distribution on the patch at three different resonant frequencies when the TM10, TM01, and TM20 modes are excited.

Conclusion

We have simulated the characteristics of a microstrip patch antenna by solving the electric field integral equation in time domain. Our numerical results were compared with measurements and the finite difference method results. The cavity model and the current distribution on the surface of the patch are used for modal analysis purposes. Additionally, different mode excitations by changing the position of the feed was demonstrated. It should be noted that this method can be applied to any arbitrary shaped microstrip patch antenna as a single element or in array configurations in transmitting and receiving modes.

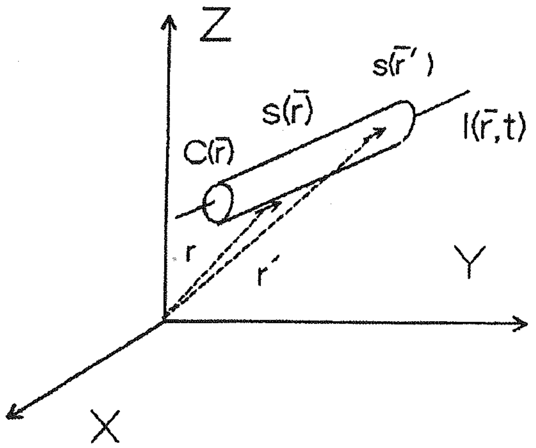

Fig (1) Geometry of the problem

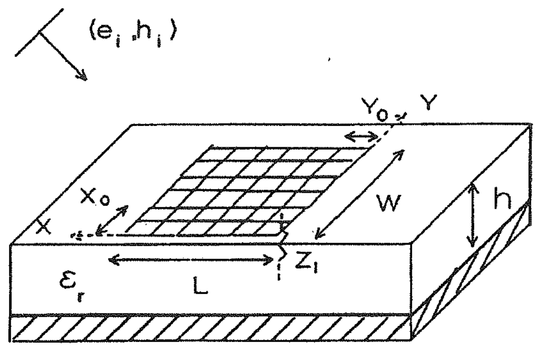

Fig (2) Wire grid model

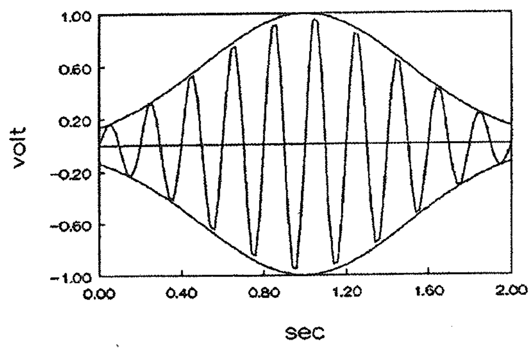

Fig (3) Shape of the excitation voltage

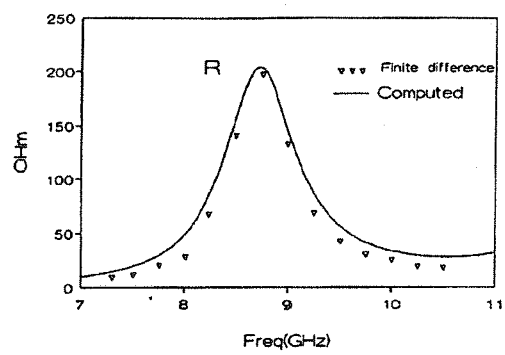

Fig (4) Input impedance (1 cm x 1 on square patch)

Continuity of the tangential electric field on the antenna surface requires

$$\hat{s} . \bar{E} (M, t) = 0 \tag{8}$$

Considering that $\bar{E}_d (M, t)$ is due to the induced current on the antenna, we get

$$\bar{E}_d (M, t) = L (I (M , t)) \tag{9}$$

Where L is the integro-differential operator derived from Mawell's equations. The integral equation for the induced current on the antenna is [4]

$$\hat{s} . \bar{E}_a (s , t) = \frac{\mu_0}{4\pi} \int_{C_0} \left(\begin{array}{l} \frac{\hat{s} . \hat{s}'}{R} \frac{\partial}{\partial t'} I(\hat{s}', t') + v \frac{\hat{s} . \bar{R}}{R^2} \frac{\partial}{\partial s'} I(\hat{s}', t') + v^2 \frac{\hat{s} . \bar{R}}{R^3} \int_0^{t'} \frac{\partial}{\partial s'} I(\hat{s}', \tau) d\tau - \\ \frac{\hat{s} . \hat{s}'^*}{R^*} \frac{\partial}{\partial t^*} I(\hat{s}', t^*) + v \frac{\hat{s} . \bar{R}^*}{R^{*2}} \frac{\partial}{\partial s'} I(\hat{s}', t'^*) + v^2 \frac{\hat{s} . \bar{R}^*}{R^{*3}} \int_0^{t'^*} \frac{\partial}{\partial s'} I(\hat{s}', \tau) d\tau \end{array} \right) dc_0$$

$$R = (| \bar{r} - \bar{r}' |^2 + a^2)^{1/2} , R^* = (| \bar{r} - \bar{r}'^* |^2 + a^2)^{1/2}$$

$$v = c / \sqrt{\varepsilon_r} , t' = t - \frac{R}{v} , t^* = t - R^* / v \tag{10}$$

Note that $\bar{E}_a$ represents the feed effect and the integration is performed on the wires that model the antenna. Finally, the resultant equation is solved by the method of moments in the time domain and the induced current on the wires is calculated [4]. By taking the Fourier transform of the induced current,the antenna parameters in the transmitting and receiving modes in a wide band of frequency could be calculated.

Comparison with Measurements bns other Methods

Three rectangular microstrip patches were analyzed and the results were compared with measurements and the finite difference method calculations. The cavity model and the current distribution on the patch were utilized for modal analysis of this antennas.

First, a 1 cm × 1 cm square patch with a dielectric substrate of $\varepsilon_r = 2.33$ and a substrate height of 1.57 mm is examined. This antenna is fed by a coaxial line and is excited by a Gaussian modulated transient voltage (Figure 3).

$$v (t) = v_0 \, e^{-a_n^2 (t - t_{max})^2} \sin 2\pi f_z (t - t_{max}) \tag{11}$$

Figure 4 compares our calculated input impedance with the finite difference results in a wide band of frequency. Figure 5 represents the comparison between the calculated reflection coefficient of the second antenna (w = 3 cm, L = 1.5 cm, h = 1. 57 cm, and ε_r = 4.5) with measurements. Good agreement between measurements and simulation could be observed. Figures 6, 7, 8, 9, and 10 display the input impedance of the same antenna at different feed positions. By changing of coax feed position, different modes (resonant frequency) of this antenna are excited. Table - 1 represents the calculated resonant frequencies of different methods. It shows that our calculations are in good agreement with the cavity and finite difference method results.

Table (1)

Mode	TM10	TM01	TM20
Cavity method (GHz)	2.357	4.714	4.714
Our method (GHz)	2.55	4.3	5.95
Finite Difference (GHz)	2.48	4.47	4.928

variable s. The radiated electric field can be calculated from [3]:

$$\bar{E}(\bar{r}, t) = -\bar{\nabla}\phi(\bar{r}, t) - \frac{\partial \bar{A}}{\partial t} \quad (2)$$

The differential operators in the above act on the observation coordinate variables. Let $\hat{s} = \hat{s}(r)$ and $\hat{s}' = \hat{s}(r')$, be the unit tangential vectors to C(r) at $\bar{r}$ and $\bar{r}'$. Then, the scalar and vector potentials could be represented as:

$$\bar{A}(r, t) = \frac{\mu_0}{4\pi} \int \frac{I(\bar{r}', t - \frac{R}{c})}{R} ds' \quad (3)$$

and

$$\phi(r, t) = \frac{1}{4\pi\varepsilon_0} \int \frac{q(\bar{r}', t - \frac{R}{c})}{R} ds'$$

The needed terms in equation (2) are:

$$\frac{\partial \bar{A}}{\partial t}(\bar{r}, t) = \frac{\mu_0}{4\pi} \int_{C(\bar{r})} \frac{\hat{S}'}{R} \frac{\partial}{\partial t} I(\bar{r}', t')\, ds'$$

and

$$\bar{\nabla}\phi = \frac{1}{4\pi\varepsilon_0} \int_{C(r)} \left[-q(\bar{r}', t') \frac{\bar{R}}{R^3} + \frac{\bar{R}}{R^2 c} \frac{\partial}{\partial s'} I(\bar{r}', t') \right] ds' \quad (4)$$

where $\hat{s} = s(\bar{r})$, $\hat{s}' = \hat{s}(\bar{r}')$, $ds' = ds(\bar{r}')$, $R = |\bar{r} - \bar{r}'|$ The unprimed coordinates $\bar{r}$ and t denote the observation point and the primed coordinates $\bar{r}'$ and $t' = t - \frac{R}{c}$ refer to the source location.

Noting that $I(\bar{r}', t') = I(\hat{s}', t')$ and $q(\bar{r}', t') = q(\hat{s}', t')$, the integro - differential equation for the induced electric field due to the filamentary current is obtained by substituting (3) and (4) in (2). Thus:

$$\bar{E}(\bar{r}, t) = -\frac{\mu_0}{4\pi} \int_{C(\bar{r})} \left[\frac{\hat{s}'}{R} \frac{\partial}{\partial t'} I(s', t') + c \frac{\bar{R}}{R^2} \frac{\partial}{\partial s'} I(s', t') - c^2 \frac{\bar{R}}{R^3} q(s', t') \right] ds' \quad (5)$$

Equation (5) is generally valid for all space and time except the source region. Since the cross section of the wire is not zero, $|\bar{r} - \bar{r}'| \geq a(r')$ and the current is assumed to flow in the central axis of the wire, the singularity of the equation is removed.

Formulation of the Rectangular Patch

The metallic patch of the antenna is modelled by wire grids situated on a dielectric substrate as shown in Figure 2. Since only the Green's function of homogeneous space is available, an equivalent dielectric medium, ε_{eff} is introduced to represent the air and dielectric layer combination [1].

$$\varepsilon_{eff} = \frac{\varepsilon_r + 1}{2} \left\{ 1 - \frac{1}{2H'} \left[\frac{\varepsilon_r - 1}{\varepsilon_r + 1}\right] \left(\ln\frac{\pi}{2} + \frac{1}{\varepsilon_r} \ln\frac{4}{\pi}\right) \right\}^{-2}$$

$w / h \leq 1.3$

$$H' = \ln\left\{ 4\frac{h}{W} + \sqrt{16\left(\frac{h}{W}\right)^2 + 2} \right\}$$

$$\varepsilon_{eff} = \frac{\varepsilon_r + 1}{\varepsilon_r - 1} + \frac{\varepsilon_r - 1}{2} \left(1 + 10\frac{h}{W}\right)^{-0555}$$

$W / h \geq 1.3$ (6)

First, assume the perfect conductor wires are illuminated by a transient electromagnetic wave. Referring to the Figure 3, the incident wave $(\bar{E}_i, \bar{H}_i)$ is reflected $(\bar{E}_r, \bar{H}_r)$ by the ground and as a result, the total field is $\bar{E}_a = \bar{E}_i + \bar{E}_r$. The total field $(\bar{E}_a)$ induces the current I (M, t) on the perfect conductor wires which generate the scattered field $(\bar{E}_d, \bar{H}_d)$. Thus, the total field is:

$$\bar{E}(M, t) = \bar{E}_a(M, t) + \bar{E}_d(M, t) \quad (7)$$

A Time Domain Analysis of a Rectangular Microstrip Patch Antenna

G. Z. Rafi
Ph.D. Student

R. Moini
Associate Professor

A. Tavakoli
Assistant Professor

Elect., Eng., Dept., Amirkabir University of Technology

Abstract

The analysis of a rectangular microstrip patch antenna using a time-domain method of moments approach is presented. The technique is capable of analyzing the antenna characteristic over a wide - band of frequency in one application. The effect of coaxial probe excitation is also considered in the calculation of the radiation properties of the antenna and its input impedance. The time domain electric field integral equation of the wire grid model is solved by the method of moments. The calculated results of the input impedance and the reflection coefficient are in good agreement with measurements in a wide band of frequency.

Introduction

Microstrip antennas are widely used in a large number of applications due to their light weight, conformability, and relatively easy and inexpensive fabrication. Numerous literature exists on analysis of microstrip antennas in frequency domain [1, 2], but, few papers have discussed the time domain characteristics of this antenna [3]. In this article, the wire grid model along with a time domain method of moments is used to compute the input impedance and radiation properties of the antenna [4].

General Theoretical Approach

The starting point of our derivation is the time domain Maxwell's equations:

$$\bar{\nabla} \times \bar{E} = -\frac{\partial \bar{B}}{\partial t}$$

$$\bar{\nabla} \times \bar{H} = \bar{J} + \frac{\partial \bar{D}}{\partial t}$$

$$\bar{\nabla} \times \bar{D} = \rho$$

$$\bar{\nabla} \times \bar{B} = 0 \qquad (1)$$

Where, ε_0 and μ_0 represent the permitivity and permeability of free space and $\bar{E}$ and $\bar{H}$ are the electric and magnetic field intensities. Furthermore, $\bar{J}$ and ρ express the volume current and charge densities of the medium respectively. In our analysis, we assume perfectly conducting bodies. Therefore, the volume current density, $\bar{J}$, is replaced by the surfaces current density, $\bar{J}_s$. Additionally, the conducting surface of the antenna are modelled by wire grids.

Fig-1 depicts a filamentary current I (r, t) flowing on the path C(r) with the length